ZIBELINE INTERNATIONAL PUBLISHING
ISSN: 1024-1752
CODEN : JERDFO

Journal of Mechanical Engineering Research and Developments (JMERD)
DOI : http://doi.org/10.26480/jmerd.05.2019.138.142

RESEARCH ARTICLE

NUMERICAL INVESTIGATION OF TANDEM EFFECTS ON BLUFF BODIES AERODYNAMICS

Ammar Ali AL-Filfily[1], Khalid M. Sowoud[2], and Abdul Wahab Hassan Khuder[3]*

[1,2,3]Middle Technical University, Baghdad, Iraq, Engineering Technical College-Baghdad, Department of Power Mechanics Engineering
**Corresponding Author Email: akhuder@toc.edu.iq*

ARTICLE DETAILS

Article History:

Received 14 June 2019
Accepted 20 July 2019
Available online 29 August 2019

ABSTRACT

Flow over bluff body is an interesting subject in recent time, which has always attractive the attention of aerodynamic researchers due to their unique flow behavior. Bluff bodies in tandem have a wide range application in engineering, such as in road vehicles (truck-trailer), railway trains, high tower building, industrial chimneys…etc. However, the non-streamed with sharp leading edges bodies exposure to high pressure drag at front face and flow separation from the leading sharp corners. Understanding the flow over these bodies led to optimize the design and control flow field by means of active or passive technique. Therefore, the main aim of the present study is to describe numerically the flow field and shielding effects of various square plates, placed coaxially as front body upstream of the square flat-faced sharp leading-edges with rounded back rear body. Analysis of 3D fluid flow behavior around the rear body alone and for the different geometrical combinations (width and gap ratios) at three Reynolds numbers based on the width of rear body in the range 1-1.8 ×105 were considered. The Computational Fluid Dynamic (CFD) using ANSYS FLUNET (19.1) with K-Ɛ turbulence model are considered for solving the governing equations for tested models. The simulated results of the flow properties such as flow stream velocity components, pressure distribution contours and pressure coefficient (Cp) around the rear body alone and front-rear body combinations, show that the optimum combination occurred at (b1/b2=0.75 and g/b2=0.5) with maximum drag reduction of 48% and 12% for the speeds 15 and 20 m/s, respectively. This reduction is due to the shielding effect of the front body that cause the separation streamlines from the front body reattachment onto or very close to the rear body shoulder. The contours of instantaneous streamline velocity patterns, pressure (Cp) and drag coefficients distributions were performed. The numerical results show a good agreement with the experimental results.

KEYWORDS

Bluff body, Numerical simulation, CFD, ANSYS FLUENT, Drag reduction.

1. INTRODUCTION

In aerodynamics, the bluff body is defined as a body having length in flow direction close or equal to that perpendicular to the flow direction (Length to height, L/D ≤ 1.0), [1], in which the flow is characterized by boundary layer separation, reattachment of the flow and forming eddies which is feed to the wake zone behind the body. All the faces are subjected to low pressure except the front face is subjected to high positive pressure. Pressure difference between the front face and rear face result in high value of pressure drag. These flow characteristics play great important in examination of several applications. Flow over bluff body is a very significant and interesting subject in recent time, which has always attractive the attention of aerodynamic researchers due to their unique flow behavior. Bluff bodies in tandem have a wide range application in engineering, such as in road vehicles (truck-trailer), railway trains, high tower building, industrial chimneys…etc. Understanding the flow over these bodies led to optimize the design and control flow field by means of active or passive technique. The net drag force on a body immersed in flow may be considered the sum of viscous (friction) drag and pressure (form) drag forces. Streamline bodies are characterized by attached flow and the drag is a result due to shear stresses (friction drag), whereas the pressures drag is relatively small. But for bluff body, the pressure drag is a resulting of distribution force normal to the body surface, this normal pressure drag may itself be considered as the sum of several distinct components, i.e.:

- Boundary layer normal-pressure drag or boundary layer pressure drag (form drag).
- Trailing vortex drag or vortex drag (induced drag).
- Wave drag (only for supersonic flow).

Pressure drag caused by boundary-layer separation (form drag) is treated in detail in present study. Most of the time the drag force is kept as small as possible, but not always. Expenditure of power is required to overcome the drag of a body in one way or another. Drag force either calculated with numerical or experimental techniques. Experimental investigations has become an important part in different researches and led to numerous discoveries, but these investigations are consume much time and more expensive. Nowadays, due to the advances in computer technology and numerical analysis, Computational Fluid Dynamic (CFD) is become more powerful tool in solving the problems that involve fluid flows.

There are several investigations dealing with the drag reduction and flow field past 3D bluff bodies by implement numerical and experimental studies. Khalid et al. [3] carried out experimental investigation the effect of D-shapes and square plat as a front body placed upstream of square flat-face, sharp-corners rear body. Remarkable drag reduction was observed for certain combinations, namely the width (b1/b2) and gab (g/b2) ratios. Xuyoug Ying et al. [4] examined in detail, the effect of various simulation parameters, such as mesh quality, turbulence model on the unsteady flow around a rectangular cylinder at Re=21400, using 2D model and 3D large eddy simulation (LES). The results show that for a rectangular cylinder with aspect ratio B/D=2 to 10, the CD and CL decrease with increasing aspect ratio. A.K. Saha et al. [5] studied numerically the flow characteristics such as vortices and transition in the wake of a square cylinder. Numerical results showed that the transition take place at Reynolds number between 150 to175. Veeralkumar Thakur et al. [6] studied the flow behavior around rectangular, radial rectangular and bullet shaped bodies using (CFD). The study indicate that bullet shape body is closed to streamline shape and is aerodynamically best among all the other cases.

The effect of splitter plate on non-circular bluff body was studied by E.Rathkrishnan [7], and found that for centerline positioning a backward splitter plate is more effective in drag reduction rather than forward splitter plate. V. Suresh et al. [8] investigated numerically the 2D flow over D-shape model with and without roughness; the analysis is carried by using CFD. The results show that a remarkable drag reduction (48%) was achieved for optimum combination with 100% roughness. S. Yagmur et al.[9], invistaged numerically and experimentally the flow in the wake zone of different profiles of bluff bodies such as triangle, square and circular at Re=5000 and 10000. Results showed that a good agreement in respect of flow patterns of vortices, velocity and streamline topology. S. Banga, [10] examined numerically the difference of rear slant angles (Ahmed body as a benchmark) and its influence on aerodynamic forces by using the CFD simulation, FLUNET (ANSYS 14). K. Koenig et al. [11] examined experimentally the effect of geometrical and gap ratios on drag and flow field of two bluff bodies, and found that a remarkable drag reduction can be achieved at certain combination (d1 /d2 and g /d2) ratio. The shielding effects of two bluff bodies (disk placed upstream of semi-infinity cylinder) in tandem by using CFD were studied by K. Filipov et al. [12]. Different geometrical configurations (diameter and gap ratios) for Reynolds number $5 \leq Re \geq 5\times105$ are studied. The drag coefficient (CD) and velocity profile numerically compared with Roshko classical experiment.

In current research, the shielding effect of two bluff bodies studied numerically by using Computational Fluid Dynamic (CFD), ANSYS FLUENT (19.1), K-Ɛ turbulence model. The effect of geometries namely, width (b1/b2) and gap (g/b2) ratios on the flow field, velocity vector control, pressure coefficient (Cp) and drag coefficient (CD) for three different velocities are investigated. The drag and pressure coefficients for each combination and for rear body alone also are calculated numerically. In addition, the effect of Reynolds number variation on drag coefficient and percentage drag reduction has been given. Validation of the numerical simulation results of drag coefficient for rear body and the others different combinations with experimental results techniques [3].

2. OBJECTIVE

The objective of this study is to find numerically the effect of geometrical parameters mainly the width and gap ratios, on drag and flow field behavior of two bluff bodies (rear and front) separated by a gap, at three different velocities. The study was carried out for rear body alone and for rear body with square plate as front body configuration. Therefore, the optimum combination can be achieved for certain combination, which resulting in remarkable drag reduction was observed. The numerical results show a good agreement with the experimental results obtained by Khalid M. and E. Rathkrishnan [3].

3. METHODOLOGY

Methodologies of present work start with the model selection, identification and collection of dimensions data from the model [3].Two models were made for this study, first is D-Shaped, rear body (b2=100mm and with curvature radius is R=50mm), as shown in figure (1), second was the modified rear body configuration having an extended arm holding the forward square-plate having six different width ratios (b1/b2= 0.25, 0.37, 0.5, 0.625, 0.75 and 1.0). The extended arm is represented the parameter as "g" holding the forward square-plate model having radius "b1" and the entire extended arm is based at "b2" of the bluff body model, the gap ratio interval are (g/b2=0.25, 0.50, 0.75 and 1.0). The creation of 3D model using ANSYS software, fine mesh generation using 3D element, the computational domain and boundary conditions used are given in Figure (1) [2].

4. NUMERICAL DESIGNS AND MODELING

4.1 Mathematical models

FLUENT is a commercial flow solver package developed by ANSYS and included in the ANSYS workbench. The software contains all necessary tools needed to model fluid flow, heat transfer, and aerodynamic applications.

There are many viscous models in the FLUENT package, the present three – dimensional model used in this work utilizes the k - ε turbulence model. The more detailed descriptions for all turbulent models may be found in ANSYS FLUENT Theory's Guide [2]. The accuracy of the results depends on the length and width of the computational domain and the boundary condition. In the current work the length and width of the domain adopted by Ying et.al [4] is used to obtain reliable and accurate results. The computational domain and boundary conditions used in the present study are given in Figure (1) [2]. They are mainly consisting of three zones. The zone one, which represents inlet condition of flow, is modeled as velocity inlet with three values (15, 20, and 26) m/s.

Zone two which represent the bluff-body and wind tunnel walls are both considered as no-slip stationary walls. For the rear boundary, zone three, a pressure outlet at the same turbulence specification as the inlet is prescribed with zero gage pressure.

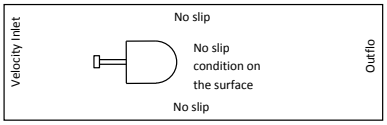

Figure 1: Computational domain and boundary conditions [4].

4.2 Mesh and Grid

In this study, a three dimension air flow around the different combination of bluff and rear bodies were estimated for different gap ratios g/b2 and b1/b2 at velocity (15, 20 and 26 m/s) using ANSYS FLUENT 19.2.The ANSYS Meshing tool is used for carrying out the meshing. Details of the mesh are as follows: Use adaptive sizing – yes, Resolution – 7, Transition – slow, Span angle center – Fine, smoothing – medium, Transition ration – 0.272, Maximum 5, Nodes : 81723, Elements : 451531.

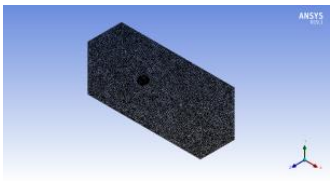

Figure 2: Computational domain and boundary conditions [Ref.4]

The ANSYS solve the continuity equation and the incompressible Navier-Stokes equations as follows:

$$\frac{\partial \bar{u}_i}{\partial x_i} = 0 \qquad \ldots (1)$$

$$\frac{\partial \bar{u}_i}{\partial t} + \frac{\partial \bar{u}_i \bar{u}_j}{\partial x_j} = \frac{1}{\rho}\frac{\partial \bar{p}}{\partial x_i} - \frac{\partial\left(\bar{u}_i \bar{u}_j - \bar{u}_i \bar{u}_j\right)}{\partial x_i} + \nu \frac{\partial^2 \bar{u}_i}{\partial x_i \partial x_j} \qquad \ldots (2)$$

Where,

t = time; xi = Cartesian coordinates; ui = velocity components; υ = kinematic viscosity

In order to solve the Navier-Stokes equations of motion (Eq.1) and continuity equation (Eq.2), the finite volume method is used in which the general transport equation for transient and 3-D flow boundary condition is given by [9]

$$\int_{CV}\left(\int_t^{t+\Delta t}\frac{\partial}{\partial t}(\rho\phi)dt\right) + \int_t^{t+\Delta t}\left(\int_A n(\rho u \emptyset)dA\right)dt = \int_t^{t+\Delta t}\left(\int_A n(\Gamma \text{grad}\emptyset)dA\right)dt + \int_t^{t+\Delta t}\left(\int_{CV} S_\emptyset dV\right)dt \qquad \ldots (3)$$

Where: Γ = diffusion coefficient; ϕ = general property and growth rate

For the purpose of calculate the drag coefficient, the force in the X-direction has found from the analysis which is nothing but the drag force. Upon substituting the drag force value in the following equation, the drag coefficient (Cd) value can be found.

$$C_d = \frac{\text{Drag force}}{0.5 \times \rho \times A \times V^2}$$

5. RESULTS AND DISCUSSION

The governing equations (1), (2) and (3) and the corresponding boundary conditions are solved numerically by using ANSYS/FLUNET (19.2).The simulated results covered the study of flow around the rear body alone (free from the front body) model, and for front-rear body combinations

with six different width ratios and four gap ratios, depend on free stream velocities (15, 20 and 26 m/s). In this study, all the computational data are calculated and compared to each other as well as some of these results are discussed with respect to the experimental data [3].

5.1 Results for Rear Body Alone

For rear body alone the numerical stream velocity contours (left column) are given in Figures 3a, 3b, and 3c. The orange area corresponds to the free-stream velocities (15, 20 and 26 m/s), respectively. The red area indicates high velocity, while the blue area shows the low velocity. The stream velocity contours clearly indicate that the wake zone behind the rear body, and consequently the pressure drag are increased as the free stream velocity increased. The boundary layer separation occurs at the leading edges of the rear body, which fed in strong, alternative eddies resulting in high wake zone behind the body, and consequently in high drag coefficient.

Figures 3d, 3e and 3f, shows the corresponding pressure coefficient contours (right column) for the three different velocities. It is clear that, the red area indicated the excess (high positive) pressure due to the stagnation of the approaching flow on the rear body front face. Whereas, the blue area indicate the suction (high negative) pressure which occurs due to the separation of boundary layers at the sharp corners resulting in large wake zone behind the body. Consequently the difference in these two pressures caused the pressure drag. The numerical values of (CDo) for the rear body alone at different velocities (V=15, 20 and 26m/s) are (1.213, 1.214 and 1.216), respectively. The numerical results with experimental data [3] are compared, for rear body alone drag coefficients (CDo) at three different velocities as shown in Table (1). These results show that the percentage differences (error) between the numerical and experimental [3], is (5%) occurs at velocity (v=15m/s). Whereas, the differences (12% and 14 %), for the other velocities 20 and 26 m/sec respectively.

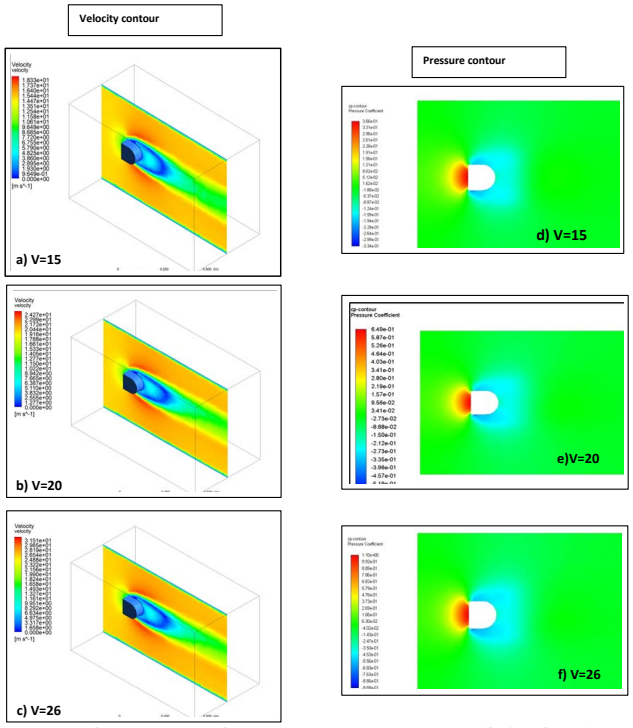

Figure 3: Flow stream velocity components contours (left column) and pressure coefficient CP contours (right column) at different velocities (V=15, 20 and 26 m/s) for the rear body only.

Table 1: Drag coefficient for rear body alone for three different velocities.

Case	Drag coefficient(C_{Do}) for rear body alone		
	V_1=15 m/s	V_2=20 m/s	V_3=26 m/s
ANSYS- FLUNET	1.213	1.214	1.216
Experimental [3]	1.28	1.39	1.42
Difference (%)	5	12	14

5.2 Results for Front-Rear Body combinations

Figure 4 shows the variation of stream velocity for front-rear body combinations, for different width ratios (b1/b2=0.25, 0.37, 0.50, 0.62, 0.75 and 1.0) and g/b2 = 0.5 at velocity 15m/s. In figure (4) shows how the geometry (i.e. width ratio) effect on the stream velocity and wake zone, red area corresponding to high velocity and low pressure, while the blue area gives low velocity and high pressure. The optimum combination is marked by [*]. Each combination will discussed and combative to each other separately.

At b1/b2=0.25, Figure 4a, for small width ratio the boundary layer separated from the front body will reattachment to the rear body face , and again separated from the rear body corners. The wake zone is started on or near the shoulders. Consequently, result in open up wake zone and high drag coefficient.

In figure 4b, b1/b2= 0.37, the flow is similar to this in b1/b2=0.25. But, it may be seen from the velocity contours that the boundary layers separation from the front body have a tendency to reattachment to the shoulder of rear body. Resulting in small wake zone compared with that take place in combination b1/b2=0.25.

For the b1/b2=0.50 and 0.62, figure 4c and 4d, these geometry combination is near to the optimum case figure 4e, (b1 */b2=0.75 and g */b2=0.5), the boundary layers separated are very close to the shoulder of rear body, but still appears unsteadiness in separated boundary layers. For combination b1/b2=0.75, figure 4e, in this case the flow is steady and the boundary layers separated from the front body are very thin and reattachment at the rear body shoulder, and consequently resulting in good shielding effect. These combination (b1 */b2=0.75 and g */b2=0.5) is the optimum case. The minimum drag coefficient (CD=0.604) achieved in this case, is lower by (48%) than the drag coefficient for rear body alone. For large combination width ratio b1/b2=1.0, figure 4f, the separated boundary layers are on the sides of the rear body. Resulting in high drag coefficient compared with the others combinations.

In Figure (5a-5f) show the pressure coefficient variation around the six different width ratios (b1/b2) for gap ratio (g/b2=0.5) at speed (V=15m/s). It can be seen that a remarkable contrast in pressure distribution between the different combinations. However, for small width ratio (b1/b2=0.25 and 0.37), it observe that the face of the rear body is exerted to high pressure (+Cp) which is represented by yellow area, due to the flow separated from the front body strike the face and become stagnation, and again separated from the face of rear body, accelerated at the upper and lower sides of the rear body, causing in pressure drop (-Cp) which is represented by a blue area as shown in figures 5a and 5b.

For a combinations (b1/b2=0.50 and 0.62), the entire rear body is subjected to low pressure coefficient and represented by blue area, while the face of front body is subjected to high pressure coefficient, as shown in figures 5c and 5d.

By compared with the optimum case (b1 */b2=0.75 and g */b2=0.5) shown in figure 5e, the rear body front face is subjected to very low pressure (-Cp) which is represented by blue area. While the other sides such as upper and lower surfaces are subjected to low pressure. This fact can be interpreted in term of boundary layers, where it separated from the front body leading edges is reattachment to the corners of the front face of rear body, resulting in small wake zone behind the rear bod and consequently in low drag coefficient.

For large width ratio (b1/b2=1.0), there is a high positive pressure (+Cp) on the face of front body and entire rear body are become under negative pressure, as shown in figure 5f. Therefore, the drag coefficient is more than the rear body alone.

The variation of drag coefficient ratio (CD/CDo) for each combination with gap ratio is plotted for Reynolds number (1-1.8) × 105 in figures (6a-6f). It is observe that the trend of drag coefficient ratio is similar for low width ratios (b1/b2=0.25 and 0.37) as illustrated in figures 6a and 6b and the drag coefficient ratio decreased as gap ratio increased. This can be explained as the separated boundary layer has a tendency to reattachment on the corners of rear body. The minimum drag coefficient can be achieved at the optimum combination (b1 */b2=0.75 and g */b2=0.5) as shown in figure 6e. Optimum shielding effect occurs at this combination, the separation boundary layers from the front body are reattachment to or very close to the rear body leading edges.

In figures (7a, 7b, 7c and 7d), show the stream velocity components contour for the optimum width ratio (b_1^*/b_2 =0.75) at different gap ratios (g/b2=0.25, 0.50, 0.75 and 1.0). It is evident that, the wake zone behind the optimum combination is steadier and smaller in size, as shown in figure (7c) when compared with the other combinations figures 7a, 7b and 7d. The reason for this behavior can be attributed to the shielding effect.
The evaluated numerical results of the minimum drag coefficient (C_D^*) for each combination (b_1^*/b_2) and the corresponding optimum gap ratio (g^*/b_2) at which it occurs for three different velocity (V=15, 20 and 26 m/s) are displayed in Table (2).

The percentage drag reduction variation with width ratio (b1/b2) is shown in figure (8), for three different velocities. The behavior exhibited is similar for all the simulated velocities. The maximum reduction in aerodynamic drag coefficient can be achieved with optimum combination (b1 */b2=0.75 and g */b2=0.5) at velocity V=15m/s. Compering with the other optimum configurations, the result is 75% more than that for the same optimum combination but at a velocity V=20m/sec. Although, the above results show that a considerable drag reduction obtained for a certain optimum (front-rear body) configurations, there are some cases other than the optimum results with less drag reduction. This can be attributed to the separated layers from the front body (square plate) are not reattach smoothly to the shoulders of the rear body, and also

The evaluated numerical results for optimum drag coefficient (C_D^*) which is obtained at corresponding velocity variation with the Reynolds number, are shown in figure (9). Further, the numerical result of (C_D^*) from the present work are compared with the experiment data [3] with slightly deviation 15% for low velocity (V=15m/s). It can be seen that, as the Reynolds number increased beyond the critical number (1-1.8) ×105, the rate of deviation increased.

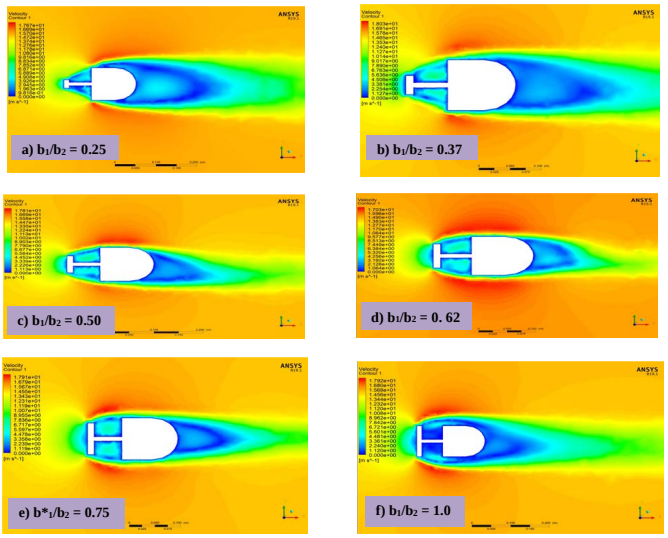

Figure 4: Flow stream velocity components contours for different width ratios (b_1/b_2=0.25, 0.37, 0.50, 0.62, 0.75 and 1.0) at gap ratio g/b_2=0.5 and velocity V=15 m/s.

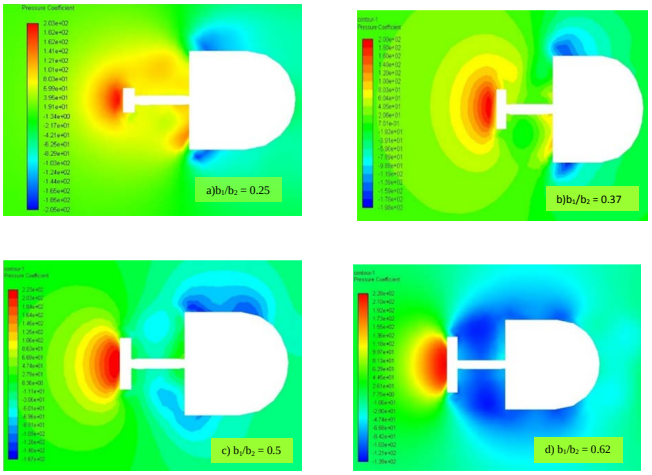

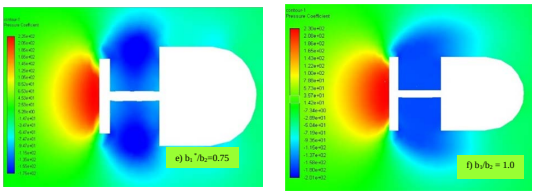

Figure 5: Pressure distribution contours for different width ratios (b_1/b_2=0.25, 0.37, 0.50, 0.62, 0.75 and 1.0) at gap ratio g/b_2=0.5 and velocity V=15 m/s.

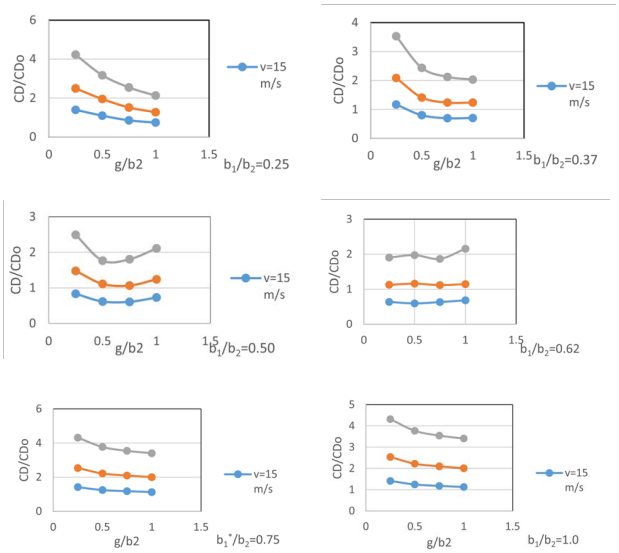

Figure 6: Shows the drag coefficient ratio for b1/b2=0.25, b1/b2=0.37, b1/b2=0.5, b1/b2=0.62, b1/b2=0.75 and b1/b2=1.0 respectively for different velocities

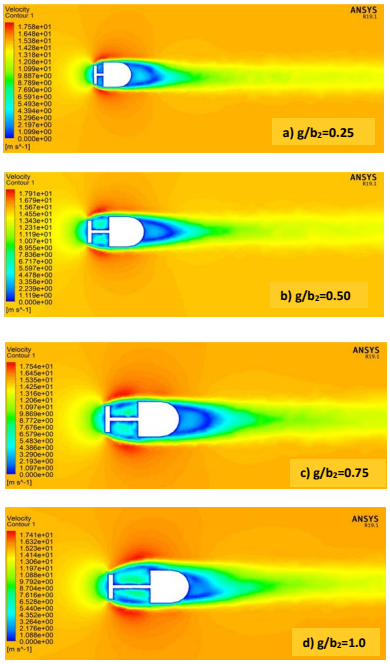

Figure 7: stream velocity components contours for b1/b2=0.75 for different gap ratio g/b2= 0.25, 0.50, 0.75 and 1.0, at velocity (V=15m/s).

Table 2: Optimum drag coefficient (C_D^*) for each combination (b_1^*/b_2) and the gap ratio (g^*/b_2) in which it occurs, for three tested speed.

No.	b_1^*/b_2	g^*/b_2	Optimum Drag coefficient (C_D^*)		
			V_1=15m/s	V_2=20m/s	V_3=26m/s
1	0.25	1.0	0.7410	1.2738	2.1284
2	0.37	0.75	0.6987	1.2402	2.1246
3	0.50	0.75	0.6087	1.0649	1.8056
4	0.62	0.75	0.6338	1.1201	1.8655
5	0.75	0.5	0.6045	1.0651	1.8036
6	1.0	0.75	1.1831	2.0997	3.2381

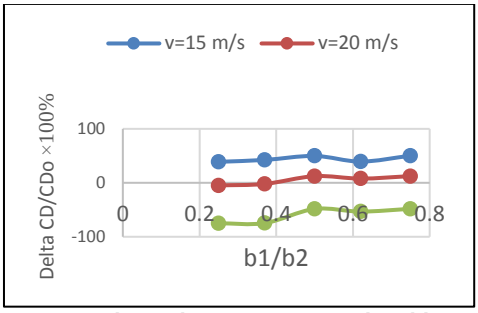

Figure 8: Percentage drag reduction variation with width ratio b1/b2 at three different velocities.

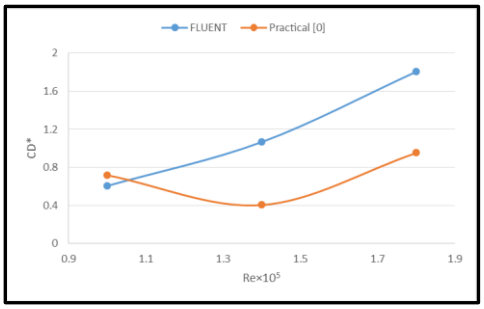

Figure 9: Comparison of variation optimum drag coefficient with Reynolds number for numerically obtained with experimental results [3].

6. CONCLUSIONS

CFD simulation results of 3D, unsteady and incompressible flow around the rear body alone and for different geometrical combinations (width and gap ratios) are discussed. The shielding effects of various square plates placed coaxially as front body upstream of the square flat-faced sharp leading-edges with rounded back rear body, at Reynolds number based on the width of rear body in the range (1-1.8) $\times 10^5$ are presented in this study. It is possible to conclude the following:

1. Based on numerical simulation, the optimum combination was achieved with ($b_1{}^*/b_2$= 0.75 and g^*/b_2= 0.5). Resulting in drag reduction 48% and 12% for the speeds 15 and 20 m/s, respectively.
2. The other investigated combinations give reduction in drag coefficient of (2-10)% ,which is consider low when compared with the drag reduction at the optimum combination.
3. Although the above conclude values show a considerable drag reduction for optimum case, there are some combinations obtained drag more than the rear body alone, resulting in negative percentage drag reduction.
4. The numerical results show that a good agreement with the experimental results that mention in[3], the difference in drag coefficient for rear body alone are 5%, 8% and 14% for the speeds 15, 20 and 26 m/s, respectively.
5. **NOMENCLATURE**
6. D: Drag force; $D = \frac{1}{2}\rho V_\infty^2 A C_D$
7. CD: Drag coefficient; $C_D = \frac{D}{1/2\,\rho\, V_\infty^2 A}$
8. CP: Pressure coefficient; $C_P = \frac{P-P_\infty}{q_\infty}$
9. q_∞: Free stream dynamic pressure; $q_\infty = \frac{1}{2}\rho V_\infty^2$
10. V_∞ : Free stream velocity
11. A: Rear body cross-sectional area; A=b2×b2
12. ρ - Air density =1.225 (kg/m3)
13. P: local static pressure on rear body
14. P_∞: Static pressure in free stream
15. b1, b2: width of front body and rear body, respectively
16. b_1^*/b_2: Optimum front body to rear body width ratio
17. g: Gap between front body and face of rear body
18. g^*/b_2: Optimum gap ratio for a given b_1^*/b_2
19. CDo: Drag coefficient of rear body alone

REFERENCES

[1] Hoerner, S.F. 1965. Fluid Dynamic Drag, 2nd Edition

[2] FLUENT. 2018. Inc., ANSYS FLUENT 19.1 Theory Guide.

[3] Khalid, M.S., Rathakrishnan, E. 1996. Front Body Effects on Drag and Flow field of a Three-Dimensional Noncircular Cylinder. AIAA Journal, 31(7), 1345-1347.

[4] Ying, X.Y., Xu, F.Y., Zhang, Z. 2012. Numerical Simulation and Visualization of flow Around Rectangular Bluff Bodies. The Seventh International Colloquium on Bluff Body Aerodynamics and Application, September 2-6.

[5] Saha, A.K., Biswas, G., Muralidhar, K. 2003. Three- dimensional study of flow past square cylinder at low Reynolds number. International Journal of Heat and Fluid Flow, 24, 54-66.

[6] Thakur, V., Yadav, T., Rajiv B. 2017. Drag Optimization of Bluff Bodies Using CFD for Aerodynamic Applications. International Journal of Computational Engineering Research (IJCER), ISSN 2250-3005, 7(4).

[7] Rathakrishnan, E. 1999. Effect of Splitter Plate on Bluff Body Drag, AIAA Journal, 37(9), 1125-1126.

[8] Suresh, V., Senthilkumar, C., Nadaraja Pillai, S., Arunvinthan, S. 2015. "Fore body Effect on Bluff Body Drag Reduction at Low Reynolds Number, International Journal of Applied Engineering Research, ISSN 0973-4562, 10(33).

[9] Yagmur, S., Dogan, S., Muharrem H., Canli, E., Ozgoren, M. 2015. Experimental and Numerical Investigation of Flow Structures around Cylindrical Bluff Bodies, Owned by the authors, published by EDP Sciences, EPJ Web of Conferences, 92, 02113.

[10] Banga, S., Zunaid, M., Ansari, N.A., Sharma, S., Dungriyal, R.S. 2015. CFD Simulation of Flow around External Vehicle: Ahmed Body, Journal of Mechanical and Civil Engineering (IOSR-JMCE) e-ISSN: 2278-1684, P-ISSN: 2320-334X, 12(4), 87-94.

[11] Koneig, K., Roshko, A. 1985. An Experimental Study of geometrical effects on the drag and flow field of two bluff bodies separated by a gap, Journal of fluid mechanics, 156, 167-204.

[12] Filipov, K., Tabakova, S. Numerical simulation of the flow around two bluff bodies separated by a gap. https://www. researchgate.net/ publication/ 313752642.